

First Energy and Angle differential Measurements of e^+e^- -pairs emitted by Internal Pair Conversion of excited Heavy Nuclei

U. Leinberger^a, E. Berdermann^a, F. Heine^b, S. Heinz^b, O. Joeres^b, P. Kienle^b,
I. Koenig^a, W. Koenig^a, C. Kozhuharov^a, A. Schröter^a, H. Tsertos^{c,1}
(ORANGE Collaboration at GSI)
C. Hofmann^d, G. Soff^d

^a Gesellschaft für Schwerionenforschung (GSI), D-64291 Darmstadt, Germany

^b Technical University of Munich, D-85748 Garching, Germany

^c University of Cyprus, CY-1678 Nicosia, Cyprus

^d Inst. f. Theoretische Physik, Technical University Dresden, D-01062 Dresden, Germany

(Revised version: December 1997)

¹Corresponding author, e-mail "tsertos@alpha2.ns.ucy.ac.cy"

Dept. Nat. Science, Univ. of Cyprus, PO 537, 1678 Nicosia, Cyprus

Abstract

We present the first energy and angle resolved measurements of e^+e^- -pairs emitted from heavy nuclei ($Z \geq 40$) at rest by internal pair conversion (IPC) of transitions with energies of less than 2 MeV as well as recent theoretical results using the DWBA method, which takes full account of relativistic effects, magnetic substates and finite size of the nucleus. The 1.76 MeV E0 transition in ^{90}Zr (^{90}Sr source) and the 1.77 MeV M1 transition in ^{207}Pb (^{207}Bi source) have been investigated experimentally using the essentially improved setup at the double-ORANGE β -spectrometer of GSI. The measurements prove the capability of the setup to cleanly identify the IPC pairs in the presence of five orders of magnitude higher β^- and γ background from the same source and to yield essentially background-free sum spectra despite the large background. Using the ability of the ORANGE setup to directly determine the opening angle of the e^+e^- -pairs ($\Theta_{e^+e^-}$), the angular correlation of the emitted pairs was measured within the range covered experimentally ($40^\circ \leq \Theta_{e^+e^-} \leq 180^\circ$). In the ^{90}Zr case the correlation could be deduced for a wide range of energy differences E_Δ of the pairs ($-530 \text{ keV} \leq E_\Delta \leq 530 \text{ keV}$). The ^{90}Zr results are in good agreement with recent theory. The angular correlation deduced for the M1 transition in ^{207}Pb is in strong disagreement with theoretical predictions derived within the Born approximation and shows almost isotropic character. This is again in agreement with the new theoretical results.

PACS numbers: 14.60.Cd, 23.20.En, 23.20.Ra, 29.25.Rm, 29.30.Aj

1 Introduction

Although known since the 1930's as one of the elementary decay channels of excited nuclear states with transition energies of more than $2m_e c^2 = 1.022$ MeV [1, 2], only limited theoretical and very limited experimental investigations of this process have been carried out in the following years. Theoretical results concerning the angular correlation of the e^+e^- pairs were mainly based on Born approximation and thus valid only for point-like low- Z nuclei and/or transition energies much higher than the threshold of 1.022 MeV [3, 4, 5, 6, 7, 8]. Only in the early 1990's more theoretical effort yielded results valid also for finite size nuclei and low transition energies (below twice the threshold) at least for electrical multipole transitions [9]. Correct treatment of magnetic transitions was achieved only recently [10], and the results for angular correlations are presented here.

Very few experimental results on IPC are published, and most of them on total IPC coefficients only, derived from the integral e^+ yield [11]. However, one very early experiment [12, 13] already measured the angular correlation for the 6 MeV E1 transition in ^{16}O , but without any energy measurement. This and other transitions of even higher energies in light nuclei have been measured recently [14] both energy and angle resolved. The results were in reasonable agreement with Born approximation, as expected, since this approximation should be valid for these cases. However, e^+e^- -pairs emitted via IPC from heavy nuclei are of considerable interest, since IPC is the only known source of e^+e^- -pairs with a sharp sum energy. Narrow lines with sum energies ($E_\Sigma = E_{e^+} + E_{e^-}$) in the range $500 \text{ keV} \leq E_\Sigma \leq 800 \text{ keV}$ have been found in heavy-ion experiments around the Coulomb barrier at GSI [15, 16, 17, 18, 19, 20, 21]. The angular correlation of the emitted leptons is of particular interest, since the response of the various setups depends strongly on it. Prior to this work, no data have been available. Additionally, the most recent theoretical results shown below should be tested experimentally.

2 Theory of internal pair conversion

The angular correlation of electron-positron pairs emitted by internal pair conversion (multipolarity $L > 0$) can be expressed in terms of Legendre polynomials [22]

$$\frac{d^2\beta}{dE d \cos \vartheta} = \frac{1}{2} \frac{d\beta}{dE} \left(1 + \sum_{i>0} a_i P_i(\cos \vartheta) \right). \quad (1)$$

The differential pair conversion coefficient $\frac{d\beta}{dE}$ and the anisotropy coefficients a_i are calculated numerically. The calculation is performed using DWBA, i.e., the electron and positron wave functions are taken to be the exact scattering solutions of the Dirac equation for the Coulomb potential of an extended nucleus [23]. The differential pair conversion coefficient and the anisotropy coefficients depend therefore on the nuclear charge number, as well as on the nuclear transition energy and the multipolarity and parity of the nuclear transition. Thus, the calculation goes beyond the Born approximation, where electron and positron wave functions are considered as plane waves [5]. $\frac{d\beta}{dE}$ is also tabulated in [10]. Fig. 1 shows the angular correlation for M1 pair conversion of an lead nucleus ($Z = 82$) and a transition energy of 1.77 MeV. The energy difference $E_\Delta = E_{e^+} - E_{e^-}$ amounts to 150 keV, which corresponds to the experimental data presented in this work (see Fig. 10 below). The calculation was performed assuming a point-like nucleus (dashed curve) as well as an extended nucleus (full curve). The point nucleus approximation is not very realistic for magnetic pair conversion in highly-charged nuclei since it overestimates the pair emission rate. Finally the dotted curve corresponds to the result obtained within the plane wave Born approximation [5], which displays the typical forward-peaked behaviour previously expected for the pair emission. For high nuclear charge numbers, the angular correlation deviates strongly from the Born approximation result. The pair emission occurs then nearly isotropic. This behaviour is elucidated by Fig. 2, which depicts the angular correlation, assuming a 1.77 MeV M1 transition with symmetric splitting of the transition energy on the electron and the positron and various nuclear charge numbers.

Also in the case of electric monopole pair conversion (denoted as E0 pair conversion) the angular correlation deviates from the Born approximation result if one takes full account of the nuclear charge number [22]. The angular correlation is then written as

$$\frac{d^2\eta}{dE d \cos \Theta} = \frac{1}{2} \frac{d\eta}{dE} (1 + \epsilon \cos \Theta). \quad (2)$$

Again the differential pair conversion coefficient $\frac{d\eta}{dE}$ and the anisotropy coefficient ϵ are computed numerically by employing the scattering solutions of the Dirac equation and assuming an extended nucleus. Using these Coulomb-distorted plane waves [23] internal

pair conversion results in a strong dependence on the nuclear charge number. In Fig. 3 the anisotropy coefficient is plotted versus the kinetic positron energy for the 1.76 MeV E0 transition in Zr ($Z = 40$) (full curve) and U ($Z = 92$) (dotted curve). If the nuclear charge number is increased the angular correlation starts to deviate from the Born approximation result [1] (dashed curve) and becomes more isotropic.

3 Experimental setup

As in the heavy-ion experiments [19, 24, 25], we use two identical iron-free, orange-type β^- spectrometers [26], facing each other with a common object point, at which a target wheel is placed (Fig. 4). Positrons (e^+) emitted in the backward ($\vartheta_{e^+} = 110^\circ - 145^\circ$) and electrons (e^-) emitted in the forward hemisphere ($\vartheta_{e^-} = 38^\circ - 70^\circ$) are focussed onto the corresponding lepton detectors. Each lepton detector consists of an array of high-resolution Si PIN diodes, called PAGODA. Intrinsic to this setup is the capability of focussing, at a given field setting, only a certain momentum interval of e^+ or e^- by rejecting the opposite charge. This is of major advantage because the high β^- background is suppressed completely on the e^+ -side, while the selection of only a certain band of e^- -momenta on the e^- -side enables operation with the strong sources required by the low branching ratios.

The leptons are identified by matching their momentum, derived from the hit-point on the PAGODA and the spectrometer field setting, with their energy, measured by the PIN diodes. This efficiently suppresses backgrounds due to γ rays. An additional coincidence requirement with the 511 keV annihilation radiation is thus not necessary for the e^+ identification. The momentum-energy matching in addition rejects the $\approx 25\%$ leptons backscattered from the PIN diodes almost completely, a unique feature of this setup. As mentioned above, for the lepton identification only events for which the energy-momentum relation is fulfilled are accepted, with the result that the remaining lepton misidentification is small and can be determined reliably. This is demonstrated in Fig. 5 for the case of the positron identification. As can be seen a clear signature for the focussed positrons is obtained. In such a spectrum all other particles, like electrons and γ rays scattered from the vacuum vessel walls and the spectrometer coils as well as positrons backscattered from the

detectors, result in a broad continuous background distribution which can be determined quantitatively. The situation is very similar for the case of the electron identification.

Each of the two identical lepton detection systems consists of 72 segmented, high-resolution, 1 mm thick, Si- PIN diodes which are mounted on 12 roofs, 6 detectors on each roof (see Fig. 4). Each detector chip has a trapezoidal shape (24 mm base, 16 mm top, and 16 mm height) which is tilted by $\approx 40^\circ$ relative to the spectrometer axis. Each detector is also subdivided into three electrically separated sectors, each covering an azimuthal angular range of $\Delta\phi_{lept} = 20^\circ$. A matrix readout, each roof as well as each three neighboring sectors at the same azimuthal angle to one preamplifier, records information on energy and arrival time of a lepton hitting a detector. Cooling the detectors to $\approx -25^\circ\text{C}$, the e^+e^- -sum-energy and time resolution achieved amounts to ≈ 15 keV and ≈ 4 ns (FWHM), respectively.

The opening angle of the e^+e^- -pair, $\Theta_{e^+e^-}$, is measured directly within a range of $40^\circ - 180^\circ$ in the laboratory. Using the ϕ -separation of the PAGODA's, this range can be subdivided into ten angular bins (see table 1) with centroids in the range $\Theta_{e^+e^-} = 70^\circ \dots 167^\circ$. These angular bins cover the same solid angle of 0.62 sr^2 , except the first and last, which cover only half of this value. This is due to simple combinatorics: for each of the angular bins all combinations between e^+ and e^- PAGODA columns with the same $|\Delta\phi|$ are put together. For $|\Delta\phi|=0^\circ$ and 180° only one column on the other PAGODA contributes, but for e.g. $|\Delta\phi|=20^\circ$ both signs are possible and two columns of the other PAGODA contribute to this $\Theta_{e^+e^-}$ -bin. The values given in table 1 have been calculated via a Monte Carlo simulation, which takes into account a realistic source spot size and the shadowing of the coils via ray tracing. The same code, but extended to handle the angular correlation of the emitted pairs, small-angle scattering and energy loss in the source, was also used for results shown later in this paper.

Each pagoda array covers a maximum momentum acceptance of $\Delta p/p = 30\%$ which corresponds to an energy interval of $\Delta E \sim 150$ keV at a lepton energy of 300 keV. Within this momentum interval, the full-energy peak efficiency is 10% and 11% of 4π , for electrons and positrons, respectively (see also Ref. [25]).

To cover an area in the E_Σ - E_Δ plane larger than given by the momentum acceptance of the spectrometers, the spectrometer currents are stepped up and down in a correlated

manner, where each step is done after the same live-time interval. Thus an intrinsic correction for dead time effects due to different count rates is achieved.

Under the assumption, that the θ -dependant longitudinal dispersion of the spectrometers cancels, the pair detection efficiency of the double-ORANGE setup can be written as follows:

$$\varepsilon = C_{spec}(E_{\Sigma}, E_{\Delta}, I_{spec}) \times C_{angle}(\Theta_{e^+e^-}), \quad (3)$$

where C_{spec} is the detection efficiency of the spectrometers for isotropic emission, depending on energy distribution and spectrometer current sweep, and C_{angle} depends on the angular correlation of the leptons. However, for any given angular correlation, the relative number of counts in every angular bin of the setup does not depend on energy distribution or spectrometer fields. The angular correlation can thus be deduced from the relative intensities alone. The above mentioned assumption is justified, if leptons entering the spectrometers at any accepted angle θ from the axis and passing the spectrometer will hit any of the pagoda's detectors. For a given, fixed spectrometer current this is true for the flat top of the efficiency of $\frac{\Delta p}{p} \approx 30\%$. At the edges of the flat top the efficiency drops fast to zero, and the efficiency in this case depends on θ . When the spectrometers are used in current sweep mode, the flat top region is extended over the whole acceptance range covered, and a θ dependance is present only at the steep edges.

4 Experimental results

With the setup described above we investigated the 1.76 MeV E0 transition in ^{90}Zr and the 1.77 MeV M1 transition in ^{207}Pb , using radioactive sources.

4.1 The 1.76 MeV E0 transition in ^{90}Zr

The first excited 0^+ state at 1.76 MeV of the 0^+ nucleus ^{90}Zr is forbidden for normal γ decay and it's main decay channels are internal conversion, emitting electrons with sharp energy given by the transition energy minus the e^- binding energy ($\approx 2/3$) and

internal pair conversion ($\approx 1/3$)², emitting e^+e^- -pairs with sharp sum energy given by the transition energy minus the equivalent of the pair's mass. The sum energy is thus $E_{\Sigma} = 1760 \text{ keV} - 1022 \text{ keV} = 738 \text{ keV}$. This energy can be shared arbitrarily between e^- and e^+ , leading to a broad E_{Δ} distribution. Due to final state Coulomb interaction with the nucleus' field this distribution is shifted to higher e^+ energies and thus positive E_{Δ} values. Other decay modes of this transition have been studied in detail theoretically [29, 30, 9, 10, 31] as well as experimentally [32, 11, 27, 28].

The 1.76 MeV transition decays to $\approx 30\%$ by IPC and is populated with a probability of 1.1×10^{-4} [33] by the β^- decay of ^{90}Y with a Q-Value of 2.6 MeV. Since this isotope is rather short-lived (64 h), we used a ^{90}Sr source, where ^{90}Y is produced in equilibrium by Strontium β^- decay with a Q-value of 586 keV. Thus every e^+e^- pair created via IPC decay of the first excited state of ^{90}Zr is accompanied by about 2×10^5 electrons from β^- decay. Especially the electrons from the ^{90}Sr decay cover exactly the range of investigated e^+ and e^- energies of $\approx 150 \dots 600 \text{ keV}$, determined by the low energy cutoff below 150 keV of our trigger electronics. To achieve satisfactory counting rates for a high statistics experiment, a very strong (in the order of 1 mCi) ^{90}Sr source had to be used, leading to total countrates on the e^- PAGODA of up to about 2 MHz as in the case of heavy-ion experiments. A very thin source had to be produced in order to keep broadening of the angular correlation by small-angle scattering of the outgoing leptons as small as possible. A source with $1.5 \mu\text{m}$ Mylar foil plus a $0.2 \mu\text{m}$ Aluminum (needed to keep the source at ground potential) was produced from commercially available ^{90}Sr solution³.

Using this source we collected a number of 1.3×10^5 e^+e^- -pairs in the sharp sum energy line of the IPC transition over a background of mainly chance coincidences of e^+ from IPC and β^- (Fig. 6a). However, the chance coincidence background can be determined quantitatively and subtraction yields the pure IPC spectrum (Fig. 6b). This spectrum is essentially background-free with a ratio of counts in the line (FWHM 15.5 keV) to the

² A very small part actually decays via multiple γ emission. The strongest of these branches emits two γ 's back to back [27]. There is even a report of a very weak single-gamma branch [28], made possible by coupling to the atomic shell electrons

³Our thanks to Dr. Brüchle and Co-workers, GSI Nuclear Chemistry Division, for the production of this source

rest of the spectrum of 5.7:1. The tail on the low energy side is due to a small part of not suppressed backscattered leptons on either side.

The high statistics in this experiment allows us to subdivide the data into 17 E_Δ intervals of 66 keV width and the ten opening angle bins of our spectrometer. Theory predicts for this E0 transition an angular correlation of the form

$$I(\Theta_{e^+e^-}) = a \cdot (1 + \epsilon \cos \Theta_{e^+e^-}), \quad (4)$$

where a is given by the conversion coefficient, source strength, detection efficiency and duration of the measurement. To determine the angular correlation coefficient ϵ the above given function is fitted to the measured data for each E_Δ bin (Fig 7a), multiplying the first and last bin by two to correct for the smaller solid angle (rf. section 3). However, the measured angular correlation includes also some small-angle scattering of the leptons in the source. To account for this the theoretical results were folded with small-angle scattering and the experimental response via a Monte Carlo simulation. The result of the simulation was fitted in the same manner as the measured data (Fig. 7b). Now the two values for ϵ can be compared. The effective source thickness of $550 \mu\text{g}/\text{cm}^2$ was calculated from the known thickness of the foils and with the assumption that the source material is pure. However, since the purity and the mean size of the crystallites of the active material are not well known, only a upper limit of about $1500 \mu\text{g}/\text{cm}^2$ can be given.

In Figure 8 we compare the anisotropy coefficients ϵ determined from the measurement with the theoretical calculations adapted to our experimental conditions via Monte Carlo simulation for various effective source thicknesses indicated. Even for a $1500 \mu\text{g}/\text{cm}^2$ thick source the theoretical values lie above the measured values except for very large $|E_\Delta|$ values. This is a hint that the real anisotropy coefficient might be somewhat smaller ($\approx 9\%$) than the calculated values. However, within the uncertainties of the current analysis (dominated by the uncertainty of the source thickness) theory and experiment are consistent. The anisotropy given by older Born approximation results [with $\epsilon(E_\Delta = 0) = 1$] is inconsistent with the measurement.

4.2 The 1.77 MeV M1 transition in ^{207}Pb

Using a rather weak (only a few μCi) ^{207}Bi calibration source ⁴ we were also able to measure e^+e^- -pairs from the weak IPC branch of the 1.77 MeV M1 transition in ^{207}Pb , leading to a narrow e^+e^- -sum-energy line at $E_\Sigma = 755 \text{ keV}$. Since we detected here only a few pairs per hour, the statistics of this measurement does not allow to subdivide into several E_Δ bins. Due to the low rates practically no chance coincidences occur in this measurement, and the measured e^+e^- sum energy spectrum shown in Fig. 9 is again of the same quality as that of Fig. 6b.

However, even the low statistics of this measurement allows us to subdivide into the ten opening angle bins and determine the angular correlation of the pairs. The theoretical prediction for $I(\Theta_{e^+e^-})$ is in this case more complex, but the form given in eq. 4 is the first order in a $\cos(\Theta_{e^+e^-})$ expansion of the correct result, so again the same fitting procedure can be used. As can be seen in Fig. 10, the situation is very different from the E0 case reported in the last section: while for the E0 case the intensity decreases for larger $\Theta_{e^+e^-}$ -values, in this case the intensity increases in the $\Theta_{e^+e^-}$ range covered by our setup, thus yielding a negative value of $\epsilon = -0.12 \pm 0.06$ for the anisotropy coefficient. This is in strong disagreement with the theoretical results derived using the Born approximation, but in good agreement with the most recent theoretical results (see Fig. 1).

These new results have some impact on estimates for the expected strength of the accompanying γ line, if some of the previously reported sum energy lines found in heavy ion experiments could be explained by IPC processes. According to these findings the pair efficiency of our setup is much higher for angular correlations having the pattern of the M1 case than for angular correlations derived from Born approximation. This is particularly true for lines appearing only in the 180° bin of the setup, where the Doppler shifts of the two leptons almost cancel: For this specific situation the detection efficiency is an order of magnitude larger for $\epsilon = -0.12$ than for $\epsilon = 1$. We would thus expect a factor of ten weaker γ line for $\epsilon = -0.12$ than in the old estimate [24]. Only a detailed re-analysis of the old data [24] can clarify whether IPC could be the origin of these weak lines. It should

⁴No ^{207}Bi source material was commercially available to produce a much stronger source in the same way as with ^{90}Sr

be noted in this context that recent results, obtained from high-resolution Doppler-shift spectroscopy in heavy-ion collisions at the Coulomb barrier, have indeed revealed that weak e^+e^- -sum-energy lines from IPC transitions of moving emitters can appear in the measured spectra [34].

5 Summary

The measurements presented in this work prove the capability of our setup to detect the sharp e^+e^- sum energy line of the IPC decay of excited heavy nuclei despite the several orders of magnitude more intense background of electrons and γ rays from the same source. The measurement with the ^{90}Sr source clearly shows that this is even the case for very high count rates in the MHz range on the electron detectors, as they are typical also for in-beam measurements (see e.g. Ref. [25]).

The results of the first energy and angle resolved measurements of IPC pairs —made more than 60 years after the first theoretical prediction of this decay branch— prove that Born approximation is not suitable for the treatment of IPC transitions of only a few times the threshold in heavy nuclei even for the most simple E0 case and by no means for magnetic multipole transitions. The theoretical results for the angular correlation presented here, taking into account all relativistic corrections, the finite size of the nucleus and also the magnetic substates for magnetic transitions, are in agreement with the experimental results shown in this paper. The combined theoretical and experimental efforts of our groups have thus led to a better understanding of a fundamental decay channel of excited nuclei that was assumed to be very well understood for decades.

References

- [1] J. R. Oppenheimer and L. Nedelski, Phys. Rev. **44**, 948 (1933).
- [2] J. C. Jaeger and H. R. Hulme, Roy. Soc. Proc. **148**, 708 (1935).
- [3] R. H. Dalitz, Proc. Phys. Soc. **A206**, 521 (1951).
- [4] G. K. Horton and E. Phibbs, Phys. Rev. **96**, 1066 (1954).
- [5] M. E. Rose, Phys. Rev. **76**, 678 (1949).
- [6] G. K. Horton, Proc. Phys. Soc. **60**, 60 (1943).
- [7] J. R. Oppenheimer, Phys. Rev. **60**, 164 (1941).
- [8] M. E. Rose and G. E. Uhlenbeck, Phys. Rev. **48**, 211 (1935).
- [9] Ch. Hofmann, Ph.D thesis, Johann Wolfgang Goethe-Universität Frankfurt, 1994; see also volume **53** of Physik, Verlag Harri Deutsch, Thun-Frankfurt/Main, 1995.
- [10] Ch. Hofmann and G. Soff, Atomic Data and Nuclear Data Tables **63**, 189–273 (1996).
- [11] J. S. Greenberg and M. Deutsch, Phys. Rev. **102**, 415–421 (1956).
- [12] S. Devons and G. R. Lindsey, Nature **4169**, 539 (1949).
- [13] S. Devons, G. Goldring and G. R. Lindsey, Proc. Phys. Soc. **A67**, 134–147 (1954).
- [14] O. Fröhlich, Ph.D thesis, Johann Wolfgang Goethe-Universität Frankfurt, 1995.
- [15] T. Cowan, H. Backe, K. Bethge, H. Bokemeyer, H. Folger, J.S. Greenberg, K. Sakaguchi, D. Schwalm, J. Schweppe, K.E. Stiebing, P. Vincent, Phys. Rev. Lett. **56**, 444 (1986).

- [16] E. Berdermann, F. Bosch, P. Kienle, W. Koenig, C. Kozhuharov, H. Tsertos, S. Schuhbeck, S. Huchler, J. Kemmer, and A. Schröter, Nucl. Phys. **A488**, 683c–688c (1988).
- [17] P. Kienle, Phys. Scr. **T23**, 123–130 (1988).
- [18] P. Kienle, Europhysics News **20**, 99–102 (1989).
- [19] W. Koenig, E. Berdermann, F. Bosch, S. Huchler, P. Kienle, C. Kozhuharov, A. Schröter, S. Schuhbeck, H. Tsertos, Phys. Lett. **B 218**, 12 (1989).
- [20] H. Bokemeyer, Habilitation, Johann Wolfgang Goethe-Universität Frankfurt, 1990; and GSI Report, **GSI-90-11**.
- [21] P. Salabura, H. Backe, K. Bethge, H. Bokemeyer, T.E. Cowan, H. Folger, J.S. Greenberg, K. Sakaguchi, D. Schwalm, J. Schweppe, K.E. Stiebing, Phys. Lett. **B 245**, 153 (1990).
- [22] C. R. Hofmann and G. Soff, Z. Phys. **A 354**, 417 (1996).
- [23] C. Hofmann, J. Augustin, J. Reinhardt, A. Schäfer, W. Greiner, and G. Soff, Phys. Scr. **48**, 257 (1993).
- [24] I. Koenig, E. Berdermann, F. Bosch, P. Kienle, W. Koenig, C. Kozhuharov, A. Schröter, H. Tsertos, Z. Phys. **A 346**, 153 (1993).
- [25] U. Leinberger, E. Berdermann, F. Heine, S. Heinz, O. Joeres, P. Kienle, I. Koenig, W. Koenig, A. Schröter, and H. Tsertos, Phys. Lett. **B394**, 16 (1997).
- [26] E. Moll and E. Kankeleit, Nukleonika **75**, 180 (1965).
- [27] J. Schirmer, D. Habs, R. Kroth, N. Kwong, D. Schwalm, M. Zirnbauer, C. Broude, Phys. Rev. Lett. **53**, 1897 (1984).
- [28] V. A. Zheltonovsk, V. M. Kolomiets, V. N. Kondratev, and V. B. Kharlanov, Sov. Phys. JETP **71**, 841 (1990).
- [29] B. F. Bayman, A. S. Reiner, and R. K. Sheline, Phys. Rev. **115**, 1627 (1959).

- [30] Ch. Hofmann, diploma thesis, Johann Wolfgang Goethe-Universität Frankfurt, 1989.
- [31] K. Huang, Phys. Rev. **102**, 422 (1956).
- [32] S. Bjørnholm, O. B. Nielsen, and R. K. Sheline, Phys. Rev. **115**, 1613 (1959).
- [33] C. M. Lederer and V. S. Shirley, *Tables of Isotopes*, John Wiley and Sons, New York, 1978.
- [34] S. Heinz, E. Berdermann, F. Heine, O. Joeres, P. Kienle, I. Koenig, W. Koenig, U. Leinberger, M. Rhein, A. Schröter, H. Tsertos, preprint (*nucl-ex/9706009*), Z. Phys. A (in press).

TABLES

Table 1: e^+e^- opening angle bins of the ORANGE setup

$\Delta\phi [^\circ]$	0	20	40	60	80	100	120	140	160	180
$\langle\Theta_{e^+e^-}\rangle [^\circ]$	70	73	80	90	102	116	131	145	159	167
$\Delta\Theta_{e^+e^-} [^\circ]$	± 14	± 13	± 13	± 12	± 11	± 9	± 9	± 8	± 8	± 7
$d\Omega^2 [sr^2]$	0.31	0.62	0.62	0.62	0.62	0.62	0.62	0.62	0.62	0.31

FIGURE CAPTIONS

Fig.1: Doubly differential pair conversion coefficient plotted versus the opening angle Θ of the electron-positron pair for an M1 transition in ^{207}Pb . The transition energy amounts to 1.77 MeV, the kinetic positron energy was fixed to 450 keV. The dotted line represents the Born approximation result, which is valid for small nuclear charge numbers. In contrast to this, the DWBA calculation yields a nearly isotropic distribution. One can also deduce the influence of the nuclear size (full line) which is compared to the point nucleus result (dashed line).

Fig.2: Angular correlation for a M1 transition with transition energy 1.77 MeV. The positron energy is fixed to 370 keV (symmetric splitting of the nuclear transition energy on electron and positron). In order to study the effect of the nuclear charge the angular distribution is plotted for the nuclear charge numbers $Z = 92$ (full curve), $Z = 82$ (dashed curve), $Z = 40$ (dash-dotted line), as well as for the Born approximation result (dotted line).

Fig.3: Anisotropy coefficient ϵ plotted versus the energy difference E_{Δ} for E0 conversion assuming a transition energy of 1.76 MeV and three nuclear charge numbers $Z = 0$ (Born approximation result, dashed line), $Z = 40$ (full line) and $Z = 92$ (dotted line). The $Z = 40$ curve is the prediction of the anisotropy coefficient for the E0 transition in ^{90}Zr .

Fig.4: Schematic view of the new double-Orange setup. Each of the β -spectrometers is equipped with a β -multidetector system of 72 Si (PIN) diodes (e^{\pm} -Pagodas). The forward spectrometer is surrounded by 18 position-sensitive heavy-ion detectors (PPAC), and contains a further PPAC detector in its center. Also shown is the rotating target wheel and the Ge(i) γ -ray detector. The only change made for the current experiment is that the target wheel was used in a stationary mode, on a target position of which the

radioactive sources were mounted.

Fig.5. Experimental signature of the detected positrons in the ^{90}Zr measurement. The abscissa shows the normalized difference between the momentum of the focused positrons calculated from the pulse height of the Si detectors and their momentum determined from the magnetic field of the spectrometer. Only events falling in a narrow window centered around zero are accepted in the analysis. The background is dominated by electrons from the five orders of magnitude more intense β^- rays, reaching the positron detectors after multiple scattering in the spectrometer.

Fig.6: e^+e^- -sum-energy spectrum from the ^{90}Sr source. Left part: raw spectrum, overlaid with the chance coincidence background due to the high (1...2 MHz) β^- count rate determined from not prompt coincidences. Right part: Sum energy spectrum after subtraction of chance coincidences. The small low energy tail is due to a small fraction of backscattered leptons not rejected by the lepton identification (see text). The sum energy line from the 1.76 MeV IPC decay in ^{90}Zr is measured essentially background-free despite the five orders of magnitude higher β^- background from the decay of ^{90}Sr and ^{90}Zr . The resolution is 15.5 keV (FWHM), the total content of the spectrum 1.59×10^5

Fig.7: An illustrative example of the determination of the angular correlation coefficient ϵ for both, measurement (left part) and theory (right part), which are treated in the same manner: The function $I = a(1 + \epsilon \cos \Theta_{e^+e^-})$ is fitted to the number of counts in the angular bins of the ORANGE setup at an energy difference centered at zero. The theoretical result is gained by folding the theoretical prediction with small-angle scattering in the source and the acceptance of the ORANGE setup by a Monte Carlo simulation. The error quoted in the experimental value of $\epsilon = 0.83 \pm 0.03$ is solely of statistical origin.

Fig.8: The extracted angular correlation coefficient ϵ for IPC decay of the 1.76 MeV transition in ^{90}Zr as a function of the energy difference E_Δ of the emitted e^+e^- -pairs. The

theoretical prediction (solid line) was folded with small-angle scattering in a source with a thickness of $750 \mu\text{g}/\text{cm}^2$ (dashed line) and $1500 \mu\text{g}/\text{cm}^2$ (dotted line). The points show the experimental result.

Fig.9: e^+e^- sum energy spectrum measured with a weak ^{207}Bi source. Due to the low count rates, chance coincidences of leptons from IC and β^+ decay branches are negligible. Again the sharp sum energy peak from the IPC decay of the 1.77 MeV M1 transition in ^{207}Pb is measured essentially background-free, even though a huge (five orders of magnitude larger) background of γ 's, e^- from IC and β^+ is present.

Fig.10: Measured angular distribution of the IPC line from the 1.77 MeV M1 transition in ^{207}Pb . Again the intensity in the first and last bin have been multiplied by two to account for their smaller solid angle. A fit done in the same manner as in Fig. 7 yields a negative anisotropy coefficient $\epsilon = -0.12 \pm 0.06$, i.e. the minimum of the intensity is at 90° rather than 180° .

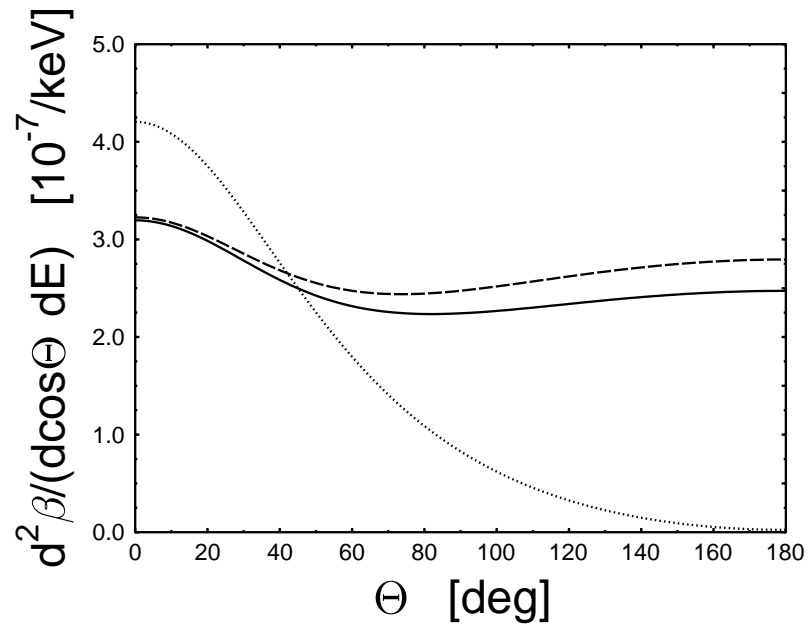


Figure 1

(U. Leinberger *et al.*, Zeitschrift für Physik A)

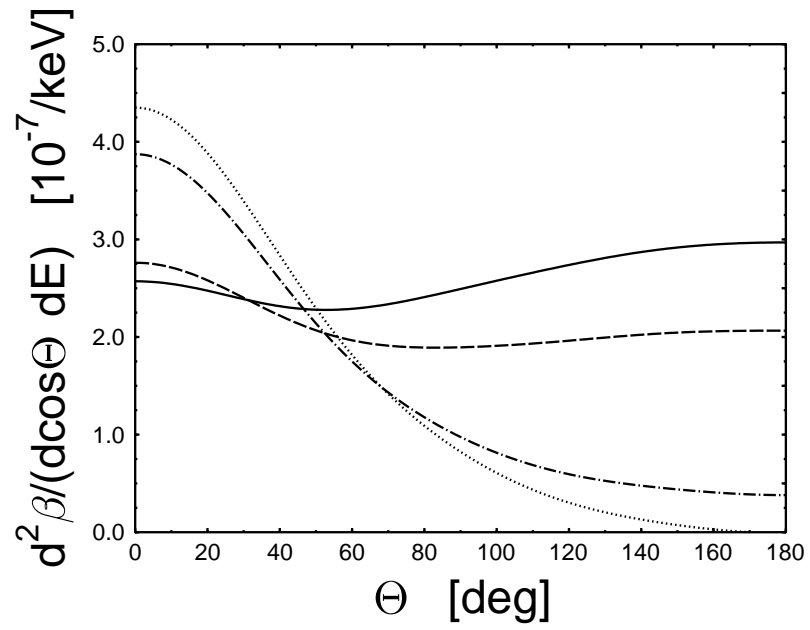


Figure 2

(U. Leinberger *et al.*, Zeitschrift für Physik A)

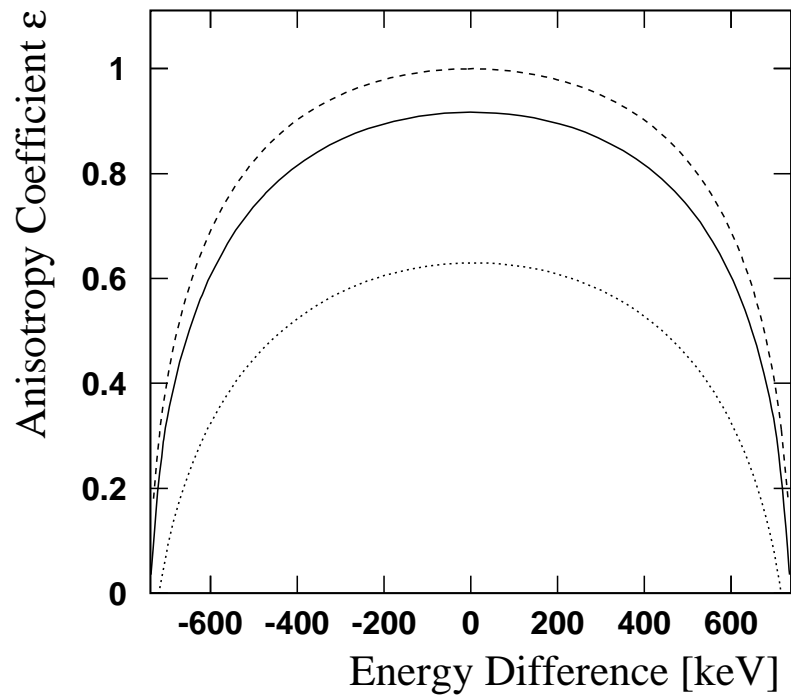


Figure 3

(U. Leinberger *et al.*, Zeitschrift für Physik A)

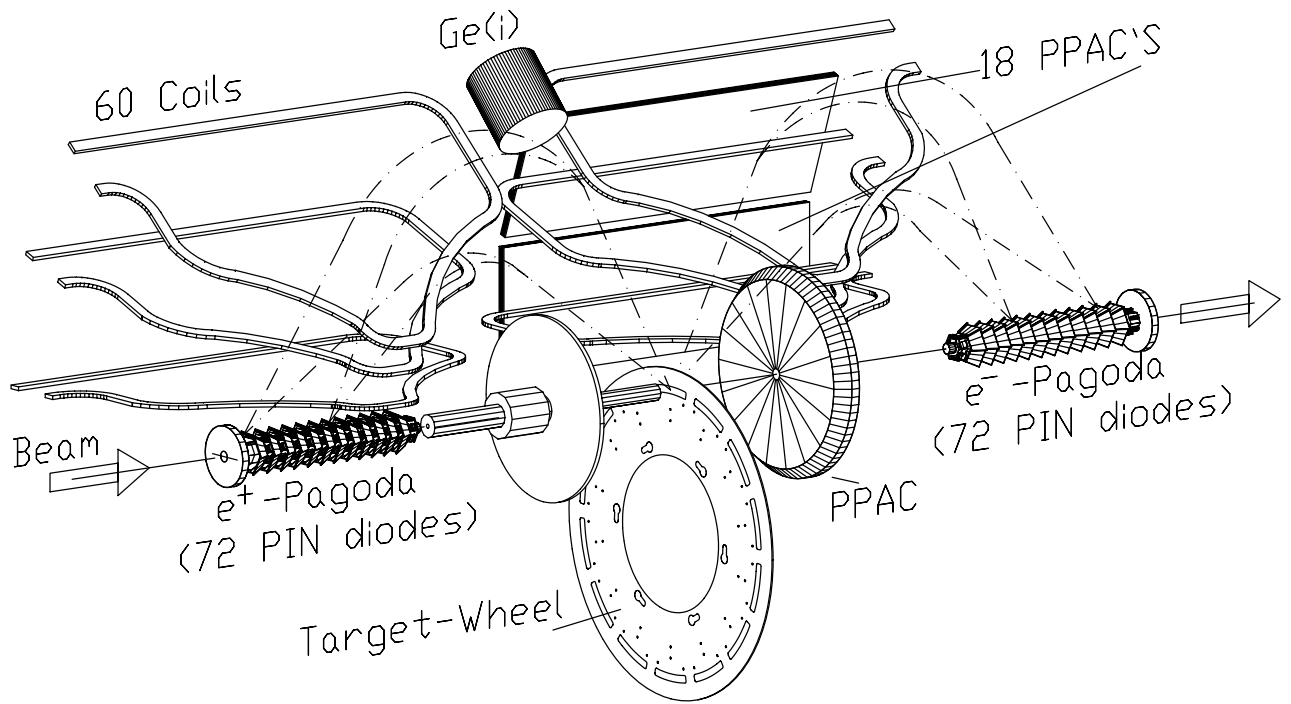


Figure 4

(U. Leinberger *et al.*, Zeitschrift für Physik A)

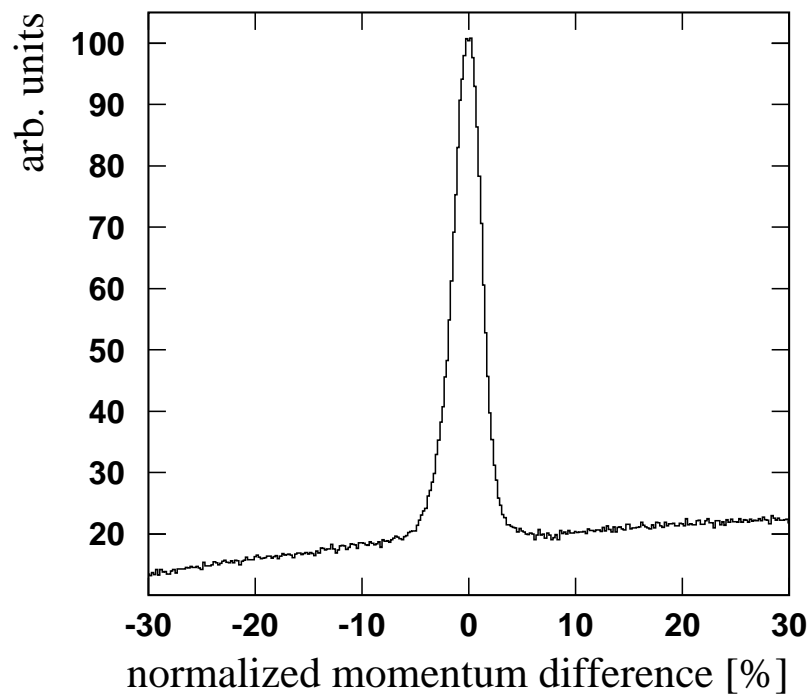


Figure 5

(U. Leinberger *et al.*, Zeitschrift für Physik A)

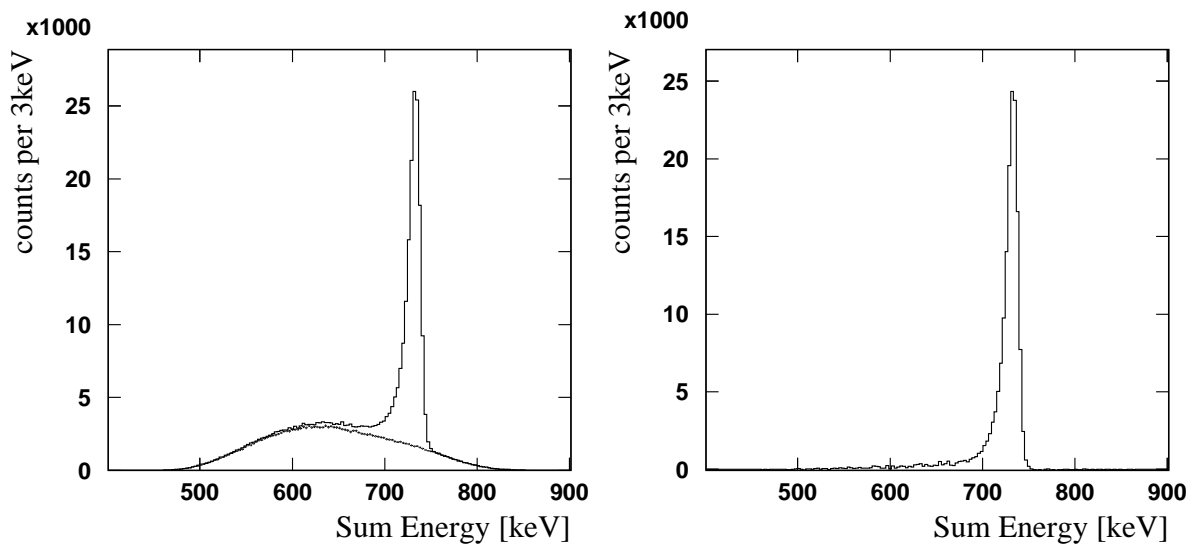


Figure 6

(U. Leinberger *et al.*, Zeitschrift für Physik A)

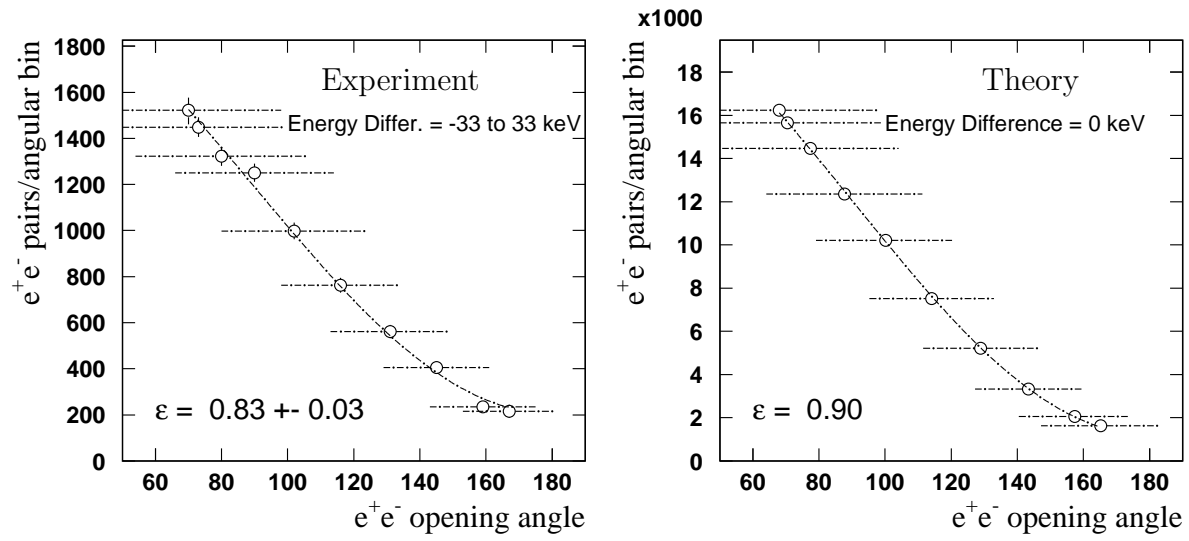


Figure 7

(U. Leinberger *et al.*, Zeitschrift für Physik A)

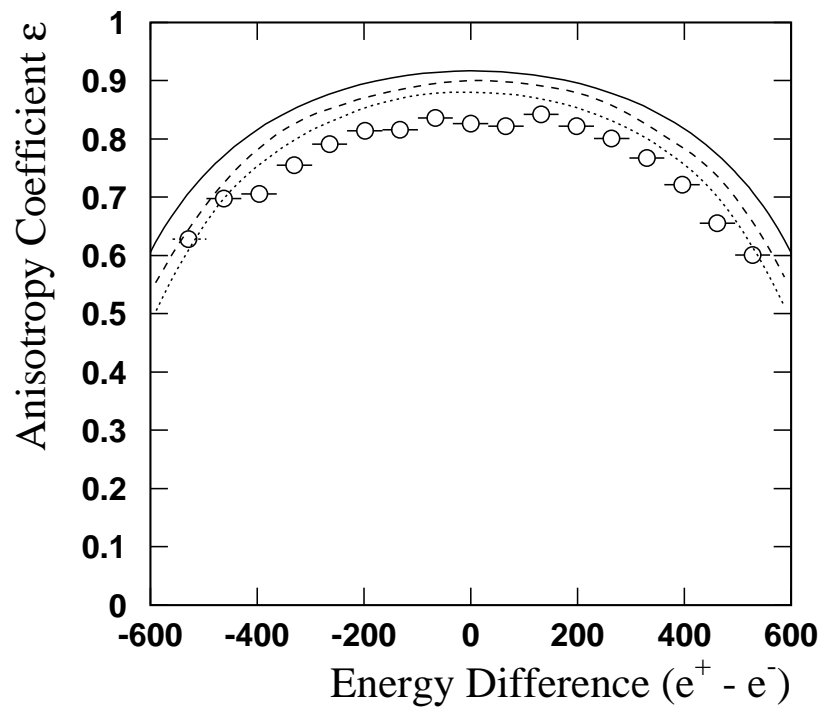


Figure 8

(U. Leinberger *et al.*, Zeitschrift für Physik A)

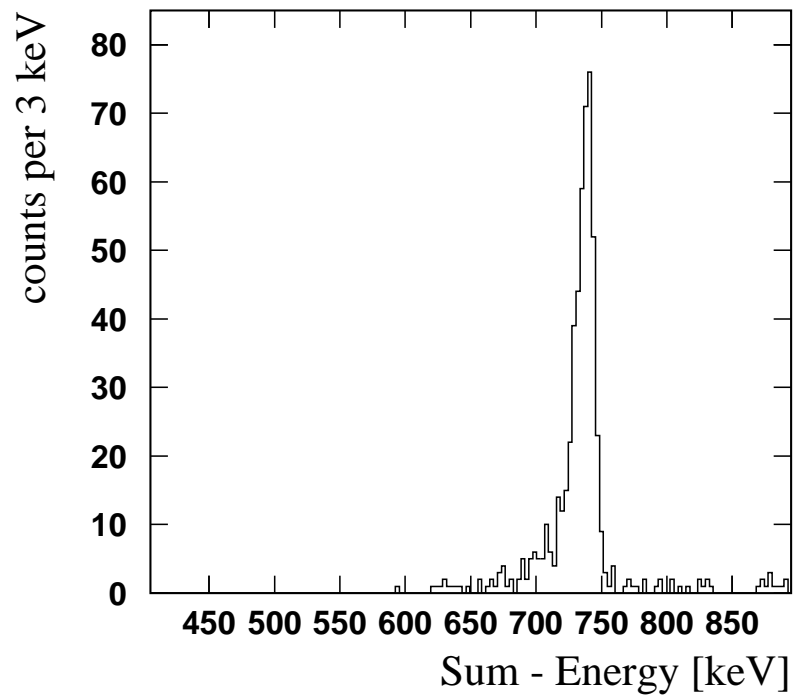


Figure 9

(U. Leinberger *et al.*, Zeitschrift für Physik A)

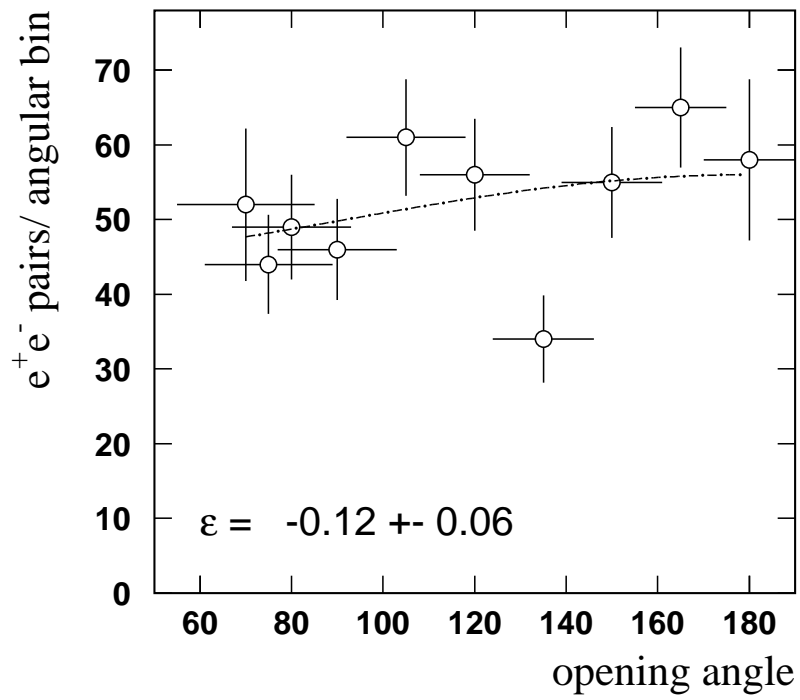


Figure 10

(U. Leinberger *et al.*, Zeitschrift für Physik A)